LETTERS

JHDM1B/FBXL10 is a nucleolar protein that represses transcription of ribosomal RNA genes

David Frescas[1], Daniele Guardavaccaro[1], Florian Bassermann[1], Ryo Koyama-Nasu[1] & Michele Pagano[1]

JHDM1B is an evolutionarily conserved and ubiquitously expressed member of the JHDM (JmjC-domain-containing histone demethylase) family[1–3]. Because it contains an F-box motif, this protein is also known as FBXL10 (ref. 4). With the use of a genome-wide RNAi screen, the JHDM1B worm orthologue (T26A5.5) was identified as a gene that regulates growth[5]. In the mouse, four independent screens have identified JHDM1B as a putative tumour suppressor by retroviral insertion analysis[6–9]. Here we identify human JHDM1B as a nucleolar protein and show that JHDM1B preferentially binds the transcribed region of ribosomal DNA to repress the transcription of ribosomal RNA genes. We also show that repression of ribosomal RNA genes by JHDM1B is dependent on its JmjC domain, which is necessary for the specific demethylation of trimethylated lysine 4 on histone H3 in the nucleolus. In agreement with the notion that ribosomal RNA synthesis and cell growth are coupled processes, we show a JmjC-domain-dependent negative effect of JHDM1B on cell size and cell proliferation. Because aberrant ribosome biogenesis and the disruption of epigenetic control mechanisms contribute to cellular transformation, these results, together with the low levels of *JHDM1B* expression found in aggressive brain tumours, suggest a role for JHDM1B in cancer development.

To begin assessing the biological function of JHDM1B, we investigated its cellular localization by using indirect immunofluorescence analysis. The results presented in Fig. 1a and Supplementary Fig. 1a show the localization of endogenous JHDM1B to the nucleolus of human cell lines (HeLa and T98G) and non-immortalized, non-transformed fibroblasts (IMR90). The nucleolar localization was confirmed by simultaneous staining with the nucleolar protein nucleophosmin/B23. Knockdown of JHDM1B by short interfering RNA (siRNA) eliminated this nucleolar signal, demonstrating the specificity of the immunostaining (Fig. 1a). JHDM1B has a putative and evolutionarily conserved nucleolar localization signal (NoLS) (Supplementary Fig. 1b). Comparison between wild-type JHDM1B and a mutant lacking the NoLS (JHDM1B(NoLS)) revealed the requirement of this basic amino-acid motif in the targeting of JHDM1B to the nucleolus (Fig. 1b). Disruption of other domains by point mutation or deletion failed to disrupt the localization of JHDM1B to the nucleolar compartment (Supplementary Fig. 2). Last, green fluorescent protein (GFP)-tagged JHDM1B localized to the nucleolus of living HeLa cells (Supplementary Fig. 3). Taken together, these data show that JHDM1B is a nucleolar protein, and its subcellular localization is dependent on the presence of a NoLS motif.

The nucleolar localization of JHDM1B, together with the presence of a CXXC zinc-finger DNA-binding domain, suggested that this protein might bind ribosomal DNA. During mitosis, rDNA-binding proteins, such as RNA polymerase I (pol I) and the pol I transcription factor UBF (upstream binding factor), remain associated with chromosomes and display discrete foci at nucleolar organizing regions (NORs)[10], which mark transcriptionally competent nucleation points for nucleoli from the previous interphase. JHDM1B localized together with UBF at NORs in mitotic cells (Supplementary Figs 4 and 5). Moreover, JHDM1B continued to localize to the nucleolar compartment after pretreatment with Triton X-100 (Supplementary Fig. 6), similar to UBF[11], suggesting stable association with rDNA.

To confirm the binding of JHDM1B to rDNA and to obtain a high-resolution map for this binding, we performed chromatin immunoprecipitation (ChIP) assays followed by quantitative real-time polymerase chain reaction (PCR) using primer pair sets that span the entire human rDNA repeat[12]. Mapping of JHDM1B binding throughout the rDNA locus showed that JHDM1B bound mainly to the transcribed region of rDNA, with particular enrichment at 8 kilobases (kb) (Fig. 1c–e). The specificity of the binding to rDNA was confirmed by the lack of JHDM1B enrichment on the *glyceraldehyde-3-phosphate dehydrogenase* (*GAPDH*) promoter and by the fact that a DNA-binding mutant, JHDM1B(CXXC), failed to bind to the 8-kb region (Fig. 1e, f). CXXC zinc-finger domains specifically recognize and bind unmethylated CpG-rich regions[13]. This binding was confirmed *in vitro* for JHDM1B[14]. CpG-island prediction by the bioinformatics program cpgplot (http://www.ebi.ac.uk/emboss/cpgplot) and previously reported biochemical studies[15] show enrichment of CpG-rich regions in rDNA over the transcribed region of rDNA (Supplementary Fig. 7), where JHDM1B binds. Thus, JHDM1B binds across the transcriptionally competent region of the rDNA repeat, with particular affinity for regions containing elevated CpG frequency.

To determine whether JHDM1B has a function in regulating rDNA transcription *in vivo*, we measured the levels of the 45S pre-ribosomal RNA by quantitative reverse transcriptase-mediated PCR (qRT–PCR). Silencing of JHDM1B by siRNA resulted in a significant increase in the expression of pre-rRNA compared with control siRNA (Fig. 2a), suggesting that JHDM1B is a repressor of rDNA transcription. Accordingly, we observed that cells expressing exogenous JHDM1B displayed a marked decrease in pre-rRNA synthesis compared with mock-transfected cells (Fig. 2b).

To investigate the domains required for JHDM1B-mediated repression of rRNA *in vivo*, we measured pre-rRNA levels in cells expressing JHDM1B mutants. Loss of the PHD finger or the F-box domain resulted in continued repression by JHDM1B, whereas loss of the NoLS or the CXXC zinc-finger blocked this transcriptional repression (Fig. 2b). We also found that the JmjC histone demethylase domain was required for the transcriptional repression of rDNA by JHDM1B (Fig. 2b). Moreover, a significant portion of cells expressing JHDM1B also failed to incorporate BrUTP within the nucleolus in a JmjC-domain-dependent manner (Fig. 2c). Taken together, these data show that JHDM1B represses rDNA transcription. This

[1]Department of Pathology, NYU Cancer Institute, New York University School of Medicine, 550 First Avenue, New York, New York 10016, USA.

repression requires the NoLS motif (to allow nucleolar localization) and the CXXC zinc-finger domain (to bind DNA). In addition, the repressive activity of JHDM1B required its JmjC domain.

To investigate the requirement for the JmjC domain, we addressed previous studies showing that JHDM1A demethylates dimethylated lysine 36 on histone 3 (H3K36me2) by means of this motif[1]. We conducted an immunofluorescence analysis in HeLa cells transfected with constructs encoding JHDM1A or JHDM1B by using an antibody against H3K36me2, and we found that forced expression of JHDM1A significantly decreased the levels of H3K36me2, as reported previously[1], whereas JHDM1B had no effect (Supplementary Fig. 8). JHDM1B was also unable to produce any significant changes in the methylation status of H3K36me3, H3K9me3, H3K27me3 or H3K4me2 (Supplementary Fig. 9). In contrast, JHDM1B overexpression resulted in a significant decrease in H3K4me3 levels, and this decrease required the presence of the JmjC domain (Fig. 3a, b). The specific reduction of H3K4me3 levels by JHDM1B was confirmed by immunoblotting (Fig. 3c, d). Last, incubation of core histones with immunopurified JHDM1B confirmed *in vitro* the ability of JHDM1B to demethylate H3K4me3 (Supplementary Fig. 10). Taken together, these results demonstrate that JHDM1B is a histone demethylase that catalyses the demethylation of H3K4me3. This finding is significant because active rRNA genes are reported to display active, euchromatic features that include H3K4me3 (refs 16, 17).

Because the decrease in global H3K4me3 levels was probably due to leakage of exogenous JHDM1B into the nucleoplasm, we investigated whether local changes in H3K4 trimethylation levels occur on rDNA by using an anti-H3K4me3 antibody in ChIP analysis. Downregulation of JHDM1B resulted in an increase in H3K4me3 on rDNA, particularly in the promoter region (42.9 kb) (Fig. 3e). Accordingly, we found a significant decrease in the levels of H3K4me3 at the rDNA locus in cells ectopically expressing JHDM1B (Fig. 3f).

Interestingly, ectopic expression of JHDM1B decreased the occupancy of UBF at rDNA regions previously reported to be enriched for the protein[12] (Fig. 3g). Similarly, JHDM1B expression decreased the amount of chromatin-bound UBF in a JmjC-dependent manner, whereas depletion of JHDM1B increased the binding of UBF to chromatin (Supplementary Figs 11 and 12).

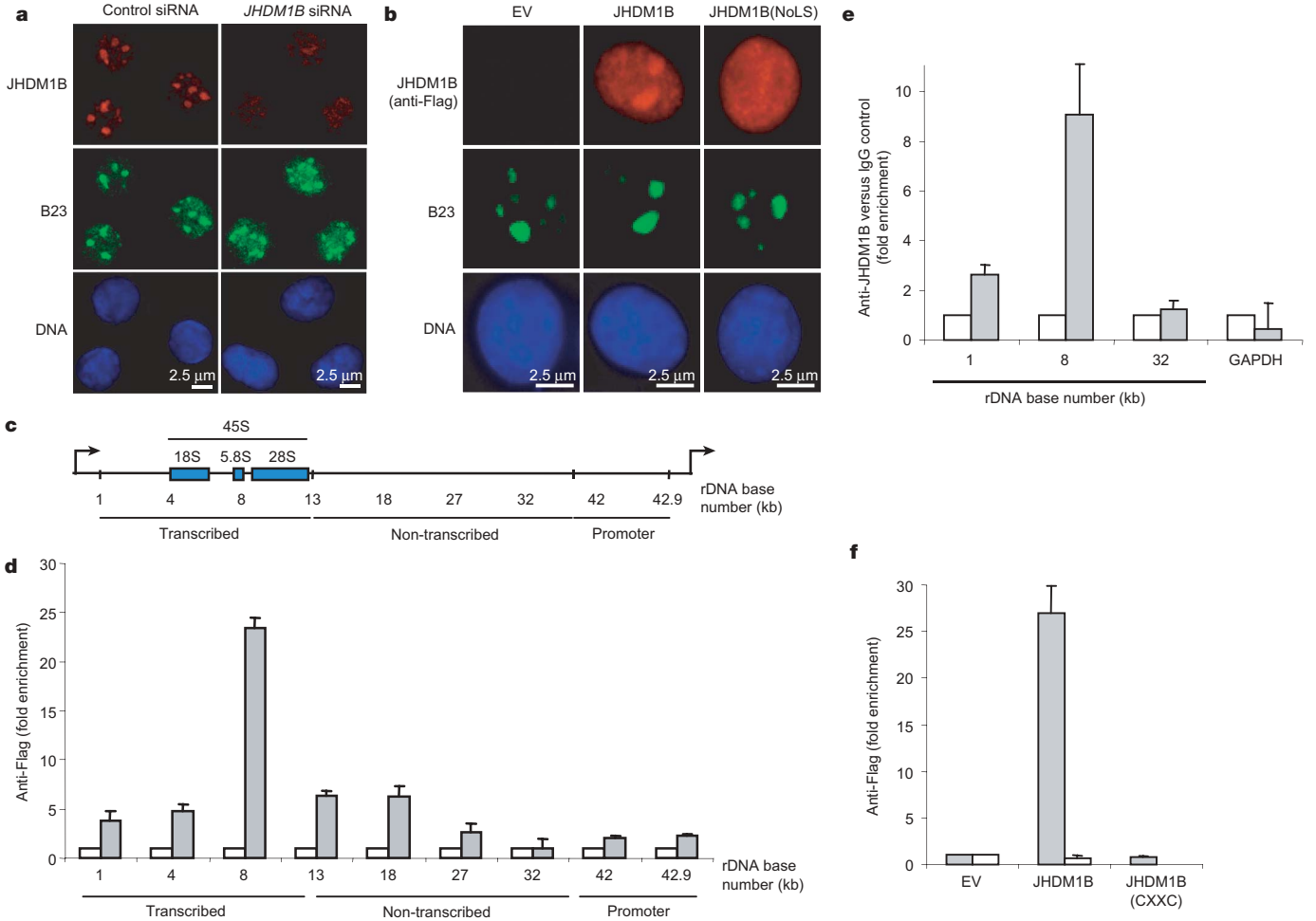

Figure 1 | JHDM1B localizes to the nucleolus and associates with rDNA. **a**, Indirect immunofluorescence analysis of endogenous JHDM1B in HeLa cells treated with control siRNA oligonucleotides or oligonucleotides targeting *JHDM1B* mRNA. Cells were stained with antibodies against JHDM1B and nucleophosmin/B23 and DAPI (to visualize DNA), as indicated. **b**, Indirect immunofluorescence analysis of HeLa cells transfected with an empty vector (EV) or constructs encoding Flag-tagged JHDM1B or JHDM1B(NoLS), as indicated. Cells were stained with an anti-Flag antibody, an antibody against B23 and DAPI. **c**, Schematic representation of a single human rDNA repeat. **d**, JHDM1B binds across the transcriptionally competent region of rDNA. Enrichment of rDNA obtained with anti-Flag antibody as determined by ChIP analysis using chromatin prepared from HeLa cells transfected with Flag–EV (open columns) or a construct encoding Flag-tagged JHDM1B (filled columns). DNA binding was quantified by real-time PCR with primer sets at indicated regions along the rDNA. The value given for the amount of PCR product present in EV-transfected cells was set at 1. **e**, Analysis of endogenous JHDM1B enrichment on rDNA and the *GAPDH* promoter by ChIP from chromatin of HeLa cells. JHDM1B enrichment (filled columns) was quantified by real-time PCR with the indicated primer sets. The value given for the amount of PCR product present from ChIP with control IgG (anti-haemagglutinin; open columns) was set as 1. **f**, ChIP experiment for enrichment of rDNA at 8 kb (filled columns) and the *GAPDH* promoter (open columns) was performed as in **d**. All error bars represent s.d. ($n = 3$).

Because the synthesis of rRNAs and cell growth are coupled processes[18], we investigated whether JHDM1B affected cell size and cell proliferation. Forward scatter analysis showed that HeLa cells exogenously expressing JHDM1B were significantly smaller than control or JHDM1B(JmjC)-expressing cells (Fig. 4a). This effect also required the NoLS and the CXXC zinc-finger domains but not the PHD domain (Supplementary Fig. 13). Cells expressing JHDM1B also incorporated about 40% less bromodeoxyuridine (BrdU) than control cells, reflecting a smaller population of cells in S phase (Fig. 4b). Conversely, cells in which JHDM1B was silenced were significantly larger than control cells and showed a 1.67-fold increase in BrdU incorporation (Fig. 4c ,d). Accordingly, JHDM1B-depleted cells proliferated at a faster rate than control HeLa cells (Fig. 4e). Taken together, these data suggest that JHDM1B-mediated modulation of rRNA gene expression influences cell growth and proliferation. Interestingly, under conditions in which rRNA production has been shown to decrease, such as during serum deprivation[19], the

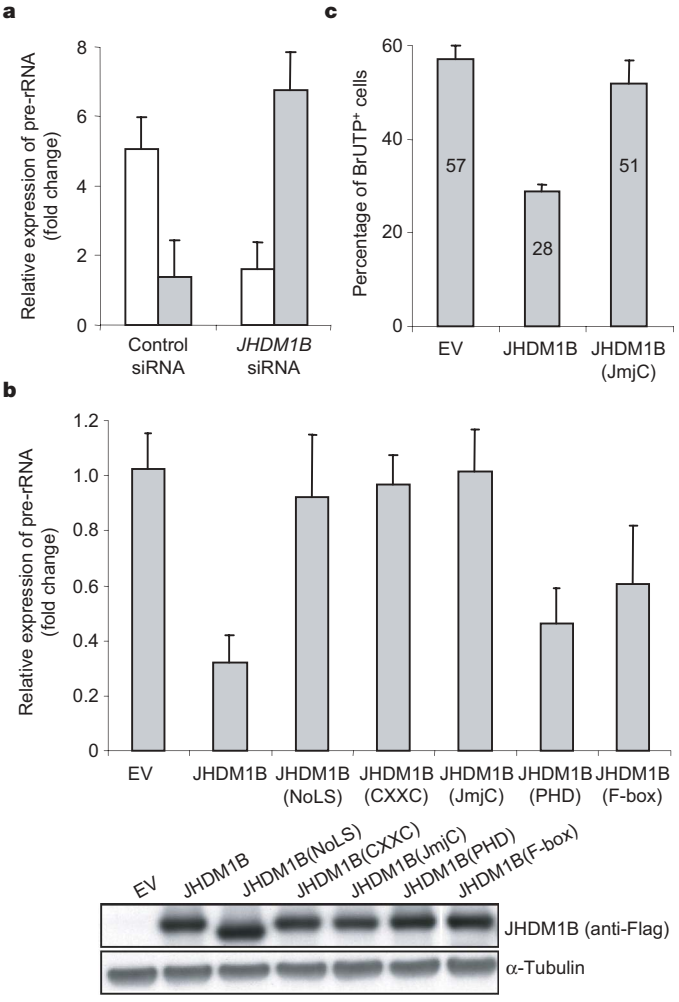

Figure 2 | JHDM1B represses transcription of rRNA genes via the JmjC domain. **a**, qRT–PCR analysis of pre-rRNA (filled columns) and *JHDM1B* mRNA (open columns) from HeLa cells transfected with siRNA targeting *JHDM1B* compared with control. The value given for the amount of pre-rRNA PCR product present in control cells was set as 1. The value given for the amount of *JHDM1B* PCR product present in control cells was set at 5. **b**, Top: qRT–PCR analysis of pre-rRNA in HeLa cells retrovirally infected with an empty vector (EV) or constructs encoding wild-type JHDM1B or the indicated mutants. The value given for the amount of pre-rRNA present in empty vector (EV) transfected cells was set as 1. Bottom: expression of JHDM1B proteins, as analysed by immunoblotting (α-tubulin was used as a loading control). **c**, Graphical representation of BrUTP incorporation in the nucleolus of HeLa cells transfected with EV or constructs encoding JHDM1B or JHDM1B(JmjC). All error bars represent s.d. ($n = 3$).

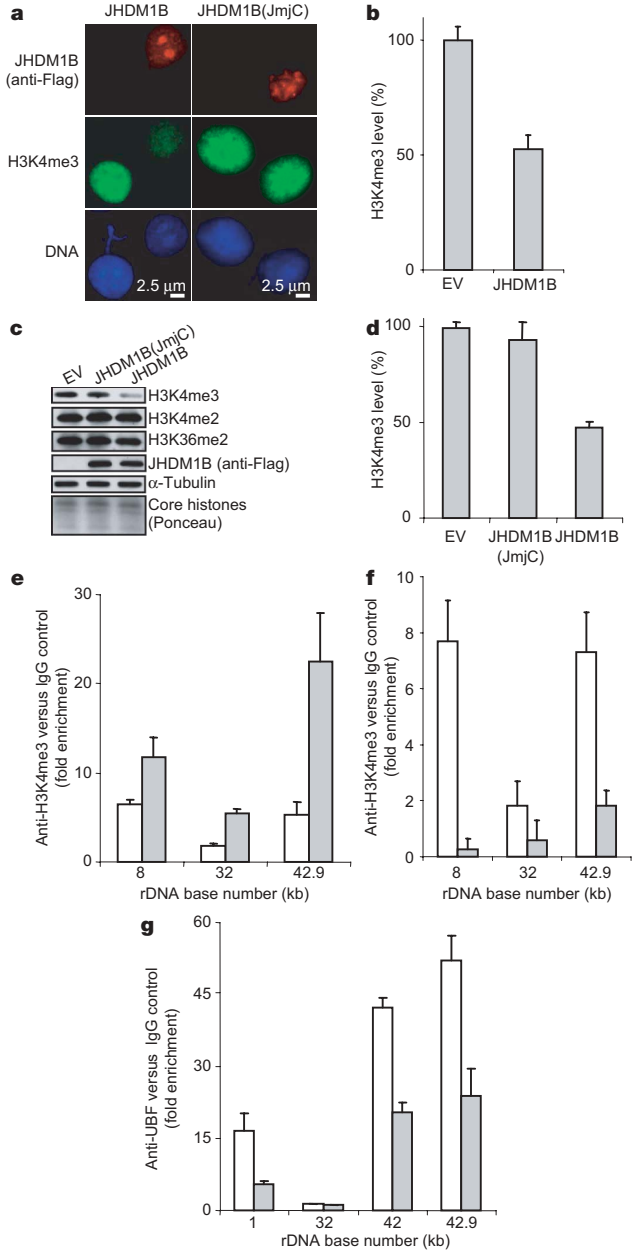

Figure 3 | JHDM1B demethylates H3K4me3 on the rDNA locus. **a**, Indirect immunofluorescence analysis of H3K4me3 levels in HeLa cells transfected with vectors encoding JHDM1B or JHDM1B(JmjC). Cells were stained with antibodies against Flag and H3K4me3, and with DAPI, as indicated. **b**, Quantification of three experiments performed as in **a**. The value given for H3K4me3 present in EV-transfected cells was set at 100%. Error bars represent s.d. ($n = 3$). **c**, Levels of methylated histone H3 in HeLa cells infected with an empty retrovirus (EV) or with retroviruses encoding JHDM1B or JHDM1B(JmjC) and analysed by immunoblotting with antibodies against the indicated proteins. The bottom panel shows core histones stained with Ponceau red. **d**, Densitometric quantification of three experiments performed as in **c**. The value given for H3K4me3 present in EV-transfected cells was set at 100%. Error bars represent s.d. ($n = 3$). **e**, HeLa cells were transfected with control siRNA (open columns) or *JHDM1B* siRNA (filled columns) oligonucleotides, and ChIPs were performed as in Fig. 1e. **f**, Analysis of H3K4me3 enrichment on rDNA, quantified as in **e**, using chromatin from 293T cells transfected with Flag–EV (open columns) or a construct encoding Flag–JHDM1B (filled columns). **g**, JHDM1B expression induces the dissociation of UBF from rDNA. Analysis of UBF enrichment on rDNA, quantified as in **e**, using chromatin from HeLa cells transfected with empty vector (open columns) or a construct encoding Flag–JHDM1B (filled columns). Error bars in **e**–**g** represent s.d. ($n = 3$).

amount of chromatin-bound JHDM1B increased, whereas serum re-addition transiently abolished this binding (Supplementary Fig. 14), suggesting that the binding of JHDM1B to rDNA is regulated by mitogens.

Actively proliferating cells transcribe high levels of rDNA and often show an increase in nucleolar number[18]. Whereas about 60% of HeLa cells possessed five or six nucleoli, cells ectopically expressing JHDM1B had a substantial nucleolar contraction, with most JHDM1B-positive cells possessing three or fewer nucleoli per cell (Fig. 4f). Consistent with the inability of JHDM1B(JmjC) and JHDM1B(NoLS) to repress rRNA expression was the observation that these mutants were unable to induce nucleolar contraction (Fig. 4f). Knockdown of JHDM1B resulted in the generation of nuclei with disorganized nucleoli; the number of nucleoli in *JHDM1B* siRNA-treated cells exceeded seven per nucleus (Figs 1a and 4g, and Supplementary Fig. 15).

A recent study has established a NOR-based index as a marker for grading and staging astrocytic lesions of the brain[20]. The number of NORs was found to rise in parallel with the grade, stage and proliferative state of the tumour. To investigate a potential involvement of JHDM1B in human cancer, we searched the Oncomine and the NIH-GEO online databases for differential *JHDM1B* expression in normal versus tumorigenic tissues[21,22]. Expression of *JHDM1B*, but not that of *JHDM1A*, was significantly decreased in the most common and the most aggressive of the primary brain tumours, glioblastoma multiform (GBM), relative to normal brain tissue (Fig. 4h and Supplementary Fig. 16). This decrease in *JHDM1B* expression was correlated with brain tumour type and tumour grade (Fig. 4i). Taken together, these results suggest that the decreased expression of *JHDM1B* might contribute to the increased cell growth/proliferation and the number of NORs in GBM tumours, possibly resulting from aberrant regulation of rRNA expression.

Thus, we show here that JHDM1B localizes to the nucleolus and provides a fundamental function for silencing rRNA genes in a manner dependent on its JmjC domain. Our findings suggest that this activity involves the demethylation of H3K4me3 at the rDNA locus, although we cannot exclude additional nucleolar, non-histone targets. Ribosome biogenesis is a highly coordinated process that ensures proper cell growth and proliferation by supporting the synthesis of proteins. Deregulation of this process has been linked to multiple forms of human disease, including cancer. Our study provides critical insight into the role of aberrant ribosome biogenesis and epigenetic mechanisms to cellular transformation. We propose JHDM1B as an addition to the list of tumour suppressors, such as p53 and pRb, that negatively regulate rRNA gene expression[18].

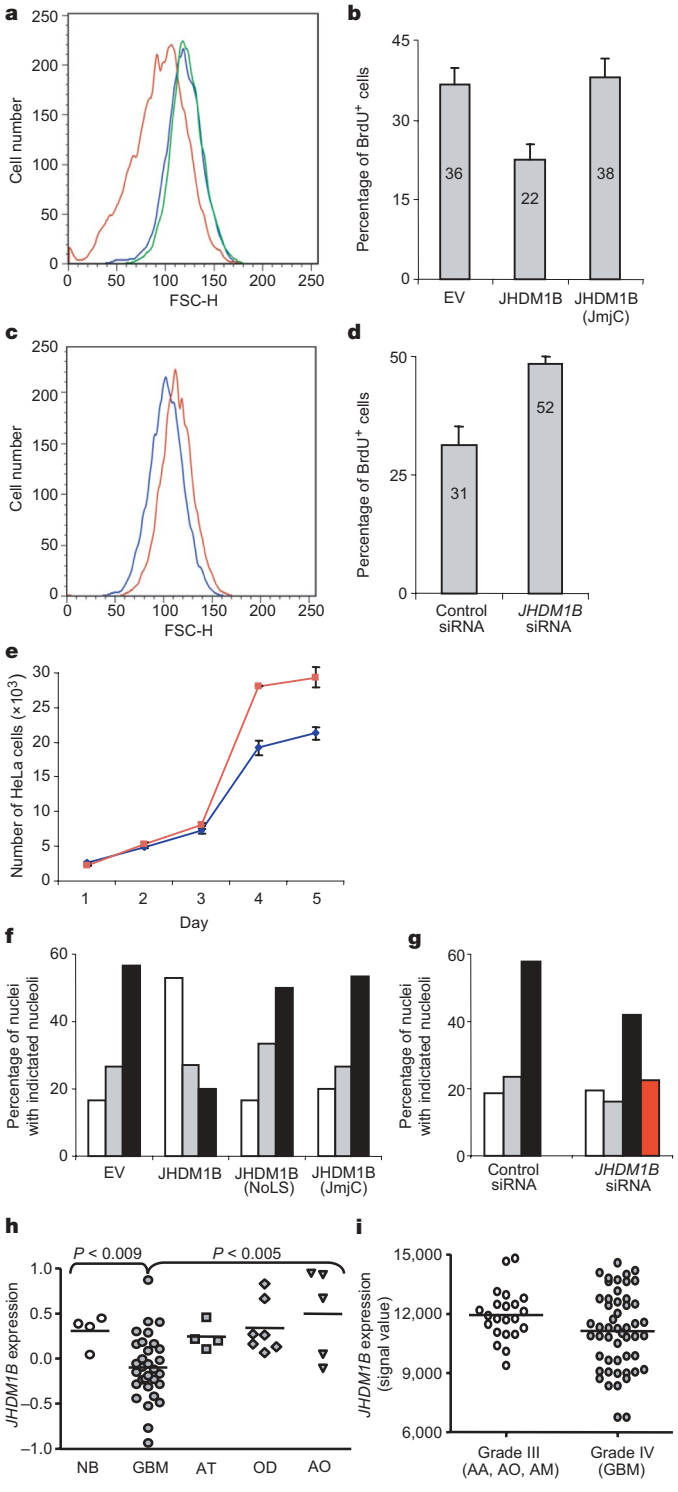

Figure 4 | JHDM1B inhibits cell growth and proliferation. **a**, Cell size was determined by fluorescence-activated cell sorting (FACS; forward scatter) in HeLa cells retrovirally infected with empty vector (blue) or constructs encoding wild-type JHDM1B (red) or JHDM1B(JmjC) (green), as indicated. **b**, Percentage of BrdU-positive HeLa cells transfected with EV or constructs encoding Flag-tagged JHDM1B or JHDM1B(JmjC). **c**, Cell size was determined by FACS (forward scatter) in HeLa cells transfected with control siRNA (blue) or *JHDM1B* siRNA (red) oligonucleotides. **d**, Percentage of BrdU-positive HeLa cells transfected as indicated. **e**, Proliferation of HeLa cells (transfected with control siRNA (blue) or *JHDM1B* siRNA (red) oligonucleotides) over a five-day period. **f**, Analysis of the number of nucleoli (determined by immunofluorescence with anti-B23 antibody) in HeLa cells transfected with EV or with constructs encoding Flag-tagged JHDM1B or the indicated JHDM1B mutants. White columns, three or fewer nucleoli; grey columns, four nucleoli; black columns, five or six nucleoli. **g**, Experiment performed as in **f** except that siRNA oligonucleotides against JHDM1B were compared with the control. White columns, three or fewer nucleoli; grey columns, four nucleoli; black columns, five or six nucleoli; red column, seven or more nucleoli. **h**, Data from ref. 21 (provided by Oncomine) reanalysed to show expression levels of *JHDM1B* in normal brain (NB), glioblastomas multiform (GBM), astrocytic tumours (AT), oligodendrogliomas (OD) and anaplastic oligoastrocytomas (AO). **i**, Data from ref. 22 (provided by NIH-GEO) reanalysed to show expression levels of *JHDM1B* in grade III and grade IV brain tumours (AA, anaplastic astrocytoma; AM, anaplastic mixed oligoastrocytoma). $P < 0.040$; $t = 1.770$. Where present, error bars represent s.d. ($n = 3$).

METHODS SUMMARY

RNA interference. HeLa cells were transfected by using HiPerFect transfection reagent (Qiagen), in accordance with the manufacturer's protocol, with either a single siRNA oligonucleotide (5′-AGGCAAGUUUAACCUCAUG-3′) or a pool of four siRNA oligonucleotides (5′-GCAAUAAGGUCACUGAUCAUU-3′, 5′-GACCUCAGCUGGACCAAUAUU-3′, 5′-GGGAGUCGAUGCUUAUUGAUU-3′ and 5′-CAGCAUAGACGGCUUCUCUUU-3′) targeting human JHDM1B (Dharmacon). Direct comparison of the pool of oligonucleotides and the single oligonucleotide (which was not present in the pool) showed identical results.

Transcription analysis by qRT–PCR. RNA was extracted with the use of the RNeasy kit (Qiagen), and reverse transcriptions were performed as described previously[12]. qRT–PCR analysis was performed in accordance with standard procedures with SYBR Green mix (Bio-Rad). Primer sequences used to detect pre-rRNA and the housekeeping gene *ARPP P0* were as reported[12]. The primer pairs used for the quantification of pre-rRNA recognize the 5′ external transcribed spacer (5′ ETS), and because the 5′ ETS is processed rapidly during transcription, it accurately reflects the rate of RNA pol I transcription[12]. The sequences used for JHDM1B were 5′-GAGGAGAAGAAGAAGGTGAAG-3′ and 5′-TTGATGGGCTGCTGGTTC-3′.

Indirect immunofluorescence. Cells were plated and cultured on chambered glass tissue-culture slides (BD Falcon) with complete medium. For immunofluorescence, cells were washed in PBS, fixed and permeabilized in 100% methanol at −20 °C for 10 min, and then incubated with the primary antibodies for 1 h at 25 °C in 0.5% Tween 20 in PBS (0.5% TBST). Slides were washed three times in 0.5% TBST for 5 min and incubated with secondary antibodies, diluted 1:1,000. 4′,6-Diamidino-2-phenylindole (DAPI; Molecular Probes) was included to reveal nuclei. Slides were washed in PBS and subsequently mounted with Aqua Poly/Mount (Polysciences). Images were acquired with a Nikon Eclipse E800 fluorescence deconvolution microscope. For pre-extraction, cells were rinsed in PBS and incubated in 0.5% Triton X-100 for 5 min on ice followed by methanol fixation at −20°C, permeabilization, and the immunofluorescence procedure described above. Fluorescence quantification was determined with ImageJ software (NIH).

Full Methods and any associated references are available in the online version of the paper at www.nature.com/nature.

Received 15 August; accepted 13 September 2007.
Published online XX 2007.

1. Tsukada, Y. *et al.* Histone demethylation by a family of JmjC domain-containing proteins. *Nature* **439,** 811–816 (2006).
2. Klose, R. J., Kallin, E. M. & Zhang, Y. JmjC-domain-containing proteins and histone demethylation. *Nature Rev. Genet.* **7,** 715–727 (2006).
3. Shi, Y. & Whetstine, J. R. Dynamic regulation of histone lysine methylation by demethylases. *Mol. Cell* **25,** 1–14 (2007).
4. Jin, J. *et al.* Systematic analysis and nomenclature of mammalian F-box proteins. *Genes Dev.* **18,** 2573–2580 (2004).
5. Pothof, J. *et al.* Identification of genes that protect the *C. elegans* genome against mutations by genome-wide RNAi. *Genes Dev.* **17,** 443–448 (2003).
6. Li, J. *et al.* Leukaemia disease genes: large-scale cloning and pathway predictions. *Nature Genet.* **23,** 348–353 (1999).
7. Suzuki, T. *et al.* New genes involved in cancer identified by retroviral tagging. *Nature Genet.* **32,** 166–174 (2002).
8. Suzuki, T., Minehata, K., Akagi, K., Jenkins, N. A. & Copeland, N. G. Tumor suppressor gene identification using retroviral insertional mutagenesis in Blm-deficient mice. *EMBO J.* **25,** 3422–3431 (2006).
9. Hwang, H. C. *et al.* Identification of oncogenes collaborating with $p27^{Kip1}$ loss by insertional mutagenesis and high-throughput insertion site analysis. *Proc. Natl Acad. Sci. USA* **99,** 11293–11298 (2002).
10. Dousset, T. *et al.* Initiation of nucleolar assembly is independent of RNA polymerase I transcription. *Mol. Biol. Cell* **11,** 2705–2717 (2000).
11. Daniely, Y., Dimitrova, D. D. & Borowiec, J. A. Stress-dependent nucleolin mobilization mediated by p53–nucleolin complex formation. *Mol. Cell. Biol.* **22,** 6014–6022 (2002).
12. Grandori, C. *et al.* c-Myc binds to human ribosomal DNA and stimulates transcription of rRNA genes by RNA polymerase I. *Nature Cell Biol.* **7,** 311–318 (2005).
13. Voo, K. S., Carlone, D. L., Jacobsen, B. M., Flodin, A. & Skalnik, D. G. Cloning of a mammalian transcriptional activator that binds unmethylated CpG motifs and shares a CXXC domain with DNA methyltransferase, human trithorax, and methyl-CpG binding domain protein 1. *Mol. Cell. Biol.* **20,** 2108–2121 (2000).
14. Koyama-Nasu, R., David, G. & Tanese, N. The F-box protein Fbl10 is a novel transcriptional repressor of c-Jun. *Nature Cell Biol.* **9,** 1074–1080 (2007).
15. Brock, G. J. & Bird, A. Mosaic methylation of the repeat unit of the human ribosomal RNA genes. *Hum. Mol. Genet.* **6,** 451–456 (1997).
16. Earley, K. *et al.* Erasure of histone acetylation by *Arabidopsis* HDA6 mediates large-scale gene silencing in nucleolar dominance. *Genes Dev.* **20,** 1283–1293 (2006).
17. Preuss, S. & Pikaard, C. S. rRNA gene silencing and nucleolar dominance: Insights into a chromosome-scale epigenetic on/off switch. *Biochim. Biophys. Acta.* **1769,** 383–392 (2007).
18. Ruggero, D. & Pandolfi, P. P. Does the ribosome translate cancer? *Nature Rev. Cancer* **3,** 179–192 (2003).
19. Zhao, J., Yuan, X., Frodin, M. & Grummt, I. ERK-dependent phosphorylation of the transcription initiation factor TIF-IA is required for RNA polymerase I transcription and cell growth. *Mol. Cell* **11,** 405–413 (2003).
20. Bukhari, M. H., Hashmi, I., Naeem, S., Abro, A. K. & Chaudhry, N. A. Use of AgNOR index in grading and differential diagnosis of astrocytic lesions of brain. *Pak. J. Med. Sci.* **23,** 206–210 (2007).
21. Bredel, M. *et al.* Functional network analysis reveals extended gliomagenesis pathway maps and three novel MYC-interacting genes in human gliomas. *Cancer Res.* **65,** 8679–8689 (2005).
22. Freije, W. A. *et al.* Gene expression profiling of gliomas strongly predicts survival. *Cancer Res.* **64,** 6503–6510 (2004).

Supplementary Information is linked to the online version of the paper at www.nature.com/nature.

Acknowledgements We thank D. Reinberg, R. Santoro, J. Skaar and J. Wysocka for suggestions and/or critically reading the manuscript; L. Busino for helping with qRT–PCR analysis; and J. Wysocka and G. David for reagents. D.F. is grateful to A. Nans. M.P. is grateful to T. M. Thor for continuous support. This work was supported by an Emerald Foundation grant to D.G., a fellowship from the German Research Foundation to F.B., a Bernard B. Levine Foundation award to R.K.-N., and grants from the NIH to M.P.

Author Contributions D.F. performed all experiments, contributed to their planning and co-wrote the manuscript. D.G. contributed to the planning of experiments and discussing and interpreting results. F.B. conducted the fluorescence-activated cell sorting analysis. R.K.-N. generated JHDM1B mutants. M.P. coordinated the study and co-wrote the manuscript. All authors discussed the results and commented on the manuscript.

Author Information Reprints and permissions information is available at www.nature.com/reprints. Correspondence and requests for materials should be addressed to M.P. (michele.pagano@nyumc.org).

METHODS

Cell culture. HeLa, T98G, 293T, GP-293 and IMR90 cells were cultured as described previously[23,24].

Antibodies. A polyclonal antibody against JHDM1B was generated by immunizing rabbits with a peptide containing amino-acid residues 800–1000 of human JHDM1B. Rabbit polyclonal antibodies were as follows: anti-Flag (F7425; Sigma), anti-haemagglutinin (anti-HA) (71-5500; Zymed), anti-di-methyl H3K36 (07-274; Upstate), anti-di-methyl H3K4 (07-030; Upstate), anti-tri-methyl H3K4 (05-745; Upstate), anti-tri-methyl H3K9 (07-523; Upstate), anti-tri-methyl H3K27 (07-449; Upstate), anti-tri-methyl H3K36 (ab9050; Abcam), anti-Alexa Fluor 568 (A11036; Molecular Probes) and anti-phospho-H3 (Ser 10) (06-570; Upstate). Mouse monoclonal antibodies were as follows: anti-M2 Flag (F3165; Sigma), anti-nucleophosmin (32-5200; Zymed), anti-UBF (sc-13125; Santa Cruz Biotechnology), anti-α-tubulin (32-2500; Zymed), anti-JHDM1B (H00084678-M09; Abnova), anti-GFP (A-11121; Molecular Probes), anti-BrdU (347580 (7580); BD) and anti-Alexa Fluor 488 (A21121; Molecular Probes).

Chromatin immunoprecipitations. ChIP assays were conducted as described previously[23]. The polyclonal antibody against JHDM1B was used for ChIP analysis of endogenous JHDM1B. anti-HA or anti-GFP antibodies were used as controls. Primer sequences for rDNA were as reported[12]. *GAPDH* sequences were: 5′-TCCACCACCCTGTTGCTGTA-3′ and 5′-ACCACAGTCCATGCCATCAC-3′.

Cell proliferation and FACS analysis. HeLa cells were transfected with siRNA oligonucleotides for two consecutive days, as described in the Methods Summary. At 48 h after the second transfection, an 80% confluent dish was trypsinized, split into five dishes and retransfected with siRNA oligonucleotides, in accordance with the long-term gene-silencing technique from the manufacturer (Qiagen). Cells were collected daily for five days and analysed by standard counting methods. FACS and forward scatter analysis were conducted as described previously[23–25].

Solubilized chromatin purification. Purification of solubilized chromatin fractions was performed as described previously[26].

BrdU and BrUTP incorporation. BrdU incorporation was performed as described previously[27]. For BrUTP incorporation, BrUTP (Molecular Probes) was added to a FuGENE 6 and 20-mM HEPES mixture (1:10) to a final concentration of 1 mM for 15 min at 25 °C, as described by Roche Molecular Biochemicals. During this short period, BrUTP specifically highlights transcriptionally active nucleoli, and no BrUTP incorporation is observed outside the nucleoli[28,29]. Slides were washed in PBS and the BrUTP–FuGENE 6 mixture was added to cells. Cells were incubated at 4 °C for 15 min, washed briefly in PBS and then incubated at 37 °C in culture medium for 5 min. Cells were processed for immunofluorescence analysis, as stated above, and an anti-BrdU antibody was used for detection. The BrdU and nucleolar-BrUTP-positive cells were analysed with standard counting methods.

Data mining. Gene expression data on *JHDM1A* and *JHDM1B* were retrieved from the Oncomine website (http://www.oncomine.org) and the National Institutes of Health (NIH) Gene expression omnibus (GEO) (http://www.ncbi.nlm.nih.gov/geo/). Data from two brain cancer studies were used for statistical calculations. Bredel *et al.*[21] includes analysis of 50 human gliomas of various histogenesis with the use of cDNA microarrays. Data were reanalysed in GraphPad software to show expression levels of *JHDM1B* and *JHDM1A*. Additional details of the study, including the pathological and clinical data, are available at Oncomine or on the *Cancer Research* journal website. Data from the second study were from an analysis of grade III and IV gliomas of various histological types[22]. These data were gathered as part of the NIH Neuroscience Microarray Consortium (http://arrayconsortium.tgen.org). Data were acquired and reanalysed with a signal value threshold of 15,000, using GraphPad software to show expression levels of *JHDM1B* and to determine *P* and one-tailed *t*-test values.

***In vitro* histone demethylation assay.** *In vitro* demethylation assays were conducted as described previously[30]. In brief, core histones were incubated with Flag-immunopurified JHDM1B from 293T cells in demethylation buffer (50 mM Tris-HCl pH 8.0, 50 mM KCl, 10 mM $MgCl_2$, 1 mM α-oxoglutarate, 40 mM $FeSO_2$, 2 mM ascorbic acid) at 37 °C. Core histones (2 μg) were incubated for 30 min with Flag-immunopurified JHDM1B in a volume of 30 μl. Reaction mixtures were analysed by western blotting. Quantification by densitometry was performed with ImageJ (NIH) software.

FRAP (fluorescence recovery after photobleaching) analysis. HeLa cells were plated, transfected with *JHDM1B–pEGFP-N1* (Clontech Laboratories) by FuGENE 6 (Roche) and observed in LabTek II chambers (Nalgene). Selective photobleaching of the nucleolus was conducted on an LSM 510 microscope (Zeiss) with laser excitation at 488 nm for GFP and a 63×, 1.2 numerical aperture, oil-immersion objective, as described previously[31]. JHDM1B–GFP fluorescence for each image in the sequence was determined with ImageJ software (NIH).

23. Busino, L. *et al.* SCFFbxl3 controls the oscillation of the circadian clock by directing the degradation of cryptochrome proteins. *Science* **316,** 900–904 (2007).
24. Dorrello, N. V. *et al.* S6K1- and βTRCP-mediated degradation of PDCD4 promotes protein translation and cell growth. *Science* **314,** 467–471 (2006).
25. Amador, V., Ge, S., Santamaria, P. G., Guardavaccaro, D. & Pagano, M. APC/C^{Cdc20} controls the ubiquitin-mediated degradation of p21 in prometaphase. *Mol. Cell* **27,** 462–473 (2007).
26. Groisman, R. *et al.* The ubiquitin ligase activity in the DDB2 and CSA complexes is differentially regulated by the COP9 signalosome in response to DNA damage. *Cell* **113,** 357–367 (2003).
27. Bashir, T., Dorrello, N. V., Amador, V., Guardavaccaro, D. & Pagano, M. Control of the $SCF^{Skp2\text{-}Cks1}$ ubiquitin ligase by the APC/C^{Cdh1} ubiquitin ligase. *Nature* **428,** 190–193 (2004).
28. Leung, A. K. *et al.* Quantitative kinetic analysis of nucleolar breakdown and reassembly during mitosis in live human cells. *J. Cell Biol.* **166,** 787–800 (2004).
29. Arabi, A. *et al.* c-Myc associates with ribosomal DNA and activates RNA polymerase I transcription. *Nature Cell Biol.* **7,** 303–310 (2005).
30. Cloos, P. A. *et al.* The putative oncogene GASC1 demethylates tri- and dimethylated lysine 9 on histone H3. *Nature* **442,** 307–311 (2006).
31. Frescas, D., Mavrakis, M., Lorenz, H., Delotto, R. & Lippincott-Schwartz, J. The secretory membrane system in the *Drosophila* syncytial blastoderm embryo exists as functionally compartmentalized units around individual nuclei. *J. Cell Biol.* **173,** 219–230 (2006).